J Solid State Electrochem (2011) 15:2341–2349
DOI 10.1007/s10008-011-1472-y

ORIGINAL PAPER

Monitoring of the electrochemical degradation of PEDOT films on gold using the bending beam method

Mária Ujvári · Mihály Takács · Soma Vesztergom · Fanni Bazsó · Ferenc Ujhelyi · Győző G. Láng

Received: 8 April 2011 / Revised: 6 June 2011 / Accepted: 7 June 2011 / Published online: 23 June 2011

Abstract Electrochemical and mechanical properties of thin poly(3,4-ethylenedioxythiophene) films deposited on gold have been investigated in aqueous sulfuric acid and sodium-sulfate solutions. It has been shown that at sufficiently positive electrode potentials, overoxidation of the polymer takes place. In some cases, only small changes could be observed in the shape of cyclic voltammograms taken in the "stability region" before and after overoxidation. In contrast to this, the impedance spectra recorded after overoxidation differed considerably from the impedance spectra of a freshly made electrode. Morphological changes of the polymer caused by overoxidation (degradation) could be detected by using the bending beam method.

Keywords PEDOT · Degradation · Bending beam method · Impedance · Stress

Introduction

In recent years, there has been great progress in research on electronic and electrochemical devices based on organic materials. Such devices are, e.g., light-emitting diodes, organic thin film transistors, solar cells, memory devices, ion-selective electrodes, microelectrode arrays, fuel cells, etc. [1–11]. The monitoring of the degradation of polymer layers is of great importance for the long term use of the devices. Among the organic conducting polymers, poly (3,4-ethylenedioxythiophene) (PEDOT) and its derivatives appear to be among the most stable organic conducting polymers currently available. Previous studies have shown that PEDOT is electroactive in aqueous solutions [12–14], and ion diffusion in PEDOT contacted by a polymer electrolyte was several orders of magnitude faster than for other conjugated polymers. On the basis of these results, studies have been performed to investigate the electrochemistry of PEDOT in more detail by using cyclic voltammetry (CV). It has been found that when the positive potential limit of the CV is extended into the region in which the overoxidation of the polymer film takes place, an oxidation peak (without a corresponding reduction peak) appears [15], but only minor changes can be observed in the properties of the cyclic voltammograms recorded in the "stability region" before and after overoxidation. The influence of the electropolymerisation potential on the properties of PEDOT films obtained in aqueous solutions has been studied in Refs. [16, 17]. It has been concluded in Ref. [16] that overoxidation of PEDOT takes place when the electropolymerisation potential is higher than +1.10 V vs. SCE, and the extent of overoxidation can be considered negligible when the potential ranges from +0.80 to +1.10 V.

According to experimental results, the mechanical properties of conductive polymers may change significantly during oxidation or reduction processes [18, 19]. Considerable stress changes in dodecylbenzenesulfonate-doped polypyrrole films have been detected by using a

Dedicated to Professor György Inzelt on occasion of his 65th birthday.

M. Ujvári · M. Takács · S. Vesztergom · F. Bazsó · G. G. Láng (✉)
Institute of Chemistry, Laboratory of Electrochemistry and Electroanalytical Chemistry, Eötvös Loránd University,
Pázmány P. s. 1/A,
1117 Budapest, Hungary
e-mail: langgyg@chem.elte.hu

F. Ujhelyi
Department of Atomic Physics,
University of Technology and Economics,
Budafoki út 8.,
1111 Budapest, Hungary

micromechanical cantilever-based sensor [20]. In these experiments, the polymer was electrochemically switched between its oxidized and neutral state by cyclic voltammetry.

The "bending beam" ("bending cantilever", "wafer curvature", etc.) method [18–30] can be effectively used in electrochemical experiments, since the changes of the stress (g_f) in a thin film or other conducting layer on one side of an insulator (e.g., glass) strip in contact with an electrolyte solution can be estimated from the changes of the radius of curvature of the strip. (Similarly, the measurement of surface stress changes is also possible [21–29].) If the potential of the electrode changes, electrochemical processes resulting in the change of g_f can take place exclusively on the metal side of the sample. The change in the film stress induces a bending moment and the strip bends. In case of a thin metal film on a substrate if the thickness of the film (t_f) is sufficiently smaller than the thickness of the plate (t_s), i.e. $t_s \gg t_f$, the change of g_f can be obtained by an expression based on a generalized form of Stoney's equation [21, 31]

$$\Delta g_f = k_i \Delta(1/R) \tag{1}$$

where k_i depends on the design of the electrode. In most cases

$$k_i = \frac{E_s t_s^2}{6 t_f (1 - \nu_s)} \tag{2}$$

where E_s, ν_s, and R are Young's modulus, Poisson's ratio, and radius of curvature of the plate, respectively. The relevant expression is more complicated, e.g., in case of a bipolymer strip [18, 19]. According to Eq. 1, for the calculation of Δg_f, the changes of the reciprocal radius $\Delta(1/R)$ of curvature of the plate must be known. The values of $\Delta(1/R) = \Delta g_f / k_i$ can be calculated, if the changes of the deflection angle $\Delta\theta$ of a laser beam mirrored by the metal layer on the plate are measured using an appropriate experimental setup as shown in Fig. 1, or the deflection of the plate is determined directly, e.g. with a scanning tunneling microscope. Thus, the bending beam method seems to be suitable for measuring the changes in the mechanical properties of PEDOT layers during oxidation/reduction, as well as for monitoring the degradation of the film during overoxidation. So far, to our knowledge, no systematic experimental study has been performed to investigate the electrochemical and mechanical properties of PEDOT modified electrodes by using the bending beam method.

The results of such an attempt are reported in the present work.

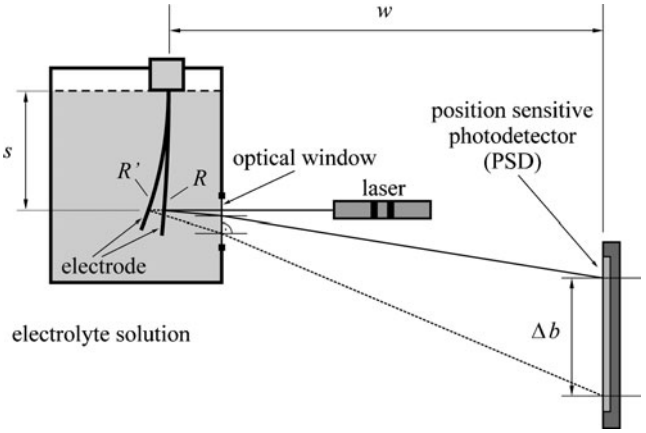

Fig. 1 Scheme of the electrochemical (optical) bending beam setup. Δb displacement of the light spot on the position-sensitive detector if the radius of curvature changes from R to R', w the distance between the electrode and the position-sensitive photodetector (*PSD*), s the distance between the solution level and the reflection point

Experimental section

1. Stress change measurements

   A He–Ne laser (Melles Griot 05-LHP-151, 1 mW, operating at a wavelength of 632.8 nm) was used in our electrochemical bending beam measuring system (Fig. 1). The displacement of the reflected beam (Δb) was measured with a position-sensitive photodetector (PSD; Hamamatsu S1300). This device was attached to a signal processing unit (Hamamatsu C4757) that can provide analog output signals proportional to the coordinates of the incident light spot. The position-sensitive detector, the laser and the electrochemical cell were assembled on an optical bench in order to avoid vibrations.

   Cantilever probes for the measurement of surface stress changes was made by evaporating a 150 nm thick gold layer on a very thin layer of titanium evaporated on one side of a glass plate (total length: l_s=60.0 mm, width: w_s=5.0 mm, thickness: t_s=149 μm, E_s=$7.09 \cdot 10^{10}$ Nm^{-2}, ν_s=0.230, and n_g=1.522, i.e., $k_i \cdot t_f$=340.4 N for the present case) after careful cleaning of the surface of the substrate. The PEDOT film on this gold layer was made by the electropolymerization method described below. An electrically isolated, thin gold layer covered the reverse side of the glass strip. This metal layer reflected the light of the He–Ne laser. The geometrical area of the electrode (in contact with the solution) was A=4.0×0.50 cm=2.0 cm^2.

   The thermostated three-electrode electrochemical cell equipped with an optical window was driven by a battery-powered potentiostat (Jaissle Model 1001 T-NC). Control voltage was supplied by a function

generator (Hewlett–Packard 3314A) or by a data acquisition card. A National Instruments 6034E DAC was used for the computer-based acquisition of the analog output signals of the PSD and the potentiostat. The software for controlling and data acquisition was developed in the National Instruments LabVIEW environment. All measurements were carried out at 25.0 °C.

For the geometry shown in Fig. 1, the following approximate equation can be derived for large R and s and small θ [21, 32–34]:

$$\Delta\left(\frac{1}{R}\right) \approx \frac{\Delta\theta}{2n_{s,i}s} \approx \frac{\Delta b}{2n_{s,i}sw} \tag{3}$$

where s is the distance between the level of the solution in the cell and the reflection point of the laser beam on the glass plate covered by a thin metal layer; w is the distance between the electrode and the PSD, Δb is the change of the position of the light spot on the PSD, and $n_{s,i}$ is the refractive index of the solution. Consequently, from Eqs. 1 and 3 at small deflections one obtains with good approximation the relation

$$\Delta g \approx \frac{k_i \Delta b}{2n_{s,i}sw} \tag{4}$$

If the actual values of k_i (or t_s,E_s, v_s,t_f), w, s, and $n_{s,i}$ are known, for the calculation of Δg only the experimental determination of Δb is necessary.

2. Solutions and electrode preparation

The gold/poly(3,4-ethylenedioxythiophene) films for electrochemical experiments were prepared by electropolymerization from 0.01 mol dm^{-3} ethylenedioxythiophene solution in 0.1 mol dm^{-3} Na_2SO_4 supporting electrolyte under galvanostatic conditions. A constant current density of 0.2 mA cm^{-2} was applied for 900 or 1,800 s. The PEDOT films were formed on the gold layer of the bending beam probes, or on both sides of gold plates used in infrared spectroscopy. Analytical grade 3,4-ethylenedioxythiophene (Aldrich), p.a. Na_2SO_4 (Fluka), and ultra-pure water (specific resistance, 18.3 MΩ cm) were used for solution preparation. The solutions were purged with oxygen-free argon (Linde 5.0). The film thickness was estimated from the charge associated with the oxidation/reduction process of the film (calculated from cyclic voltamograms), and by using the charge/film volume ratio determined earlier by direct thickness measurements (~0.24 C cm^{-2} corresponds to 1 μm thickness) [12, 35, 36].

Poly(*o*-phenylenediamine) (PPD) films were prepared by electropolymerization from 0.05 mol dm^{-3} *o*-phenylenediamine (Merck, recrystallized)+ 0.5 mol dm^{-3} H_2SO_4 solution under continuous cycling between −0.2 and +0.95 V vs. SCE (sweep rate, 25 mV s^{-1}) [37]. The film thickness was estimated by the "accordion door method" presented in [38].

Solutions used for bending beam, cyclic voltammetric and impedance measurements were prepared with ultra-pure water, and p.a. H_2SO_4 (Merck) or p.a. Na_2SO_4 (Fluka). The solutions were purged with oxygen-free argon (Linde 5.0) before use and an inert gas blanket was maintained throughout the experiments.

Refractive indexes were measured at 25.0 °C with a Zeiss PR 2 refractometer (at a wavelength of 643.8 nm (Cd C′))—0.05 mol dm^{-3} sulfuric acid solution: $n_{s,1}$= 1.3338; 0.1 mol dm^{-3} sulfuric acid solution: $n_{s,2}$= 1.3354; 0.1 mol dm^{-3} sodium-sulfate solution: $n_{s,3}$= 1.3361.

3. Cyclic voltammetry and impedance measurements

The conventional three-electrode cell configuration was used. A high surface area gold-foil (in the cell for optical measurements a spiral shaped gold wire) was arranged cylindrically around the working electrode to maintain a uniform electric field (counter electrode). The reference electrode was a saturated calomel electrode (SCE). Impedance measurements at different potentials were carried out using an Autolab PGSTAT 20 system over a frequency ranging from 5 to 50 mHz to 10 to 40 kHz. The impedance was measured at 60–80 discrete frequencies in the frequency region investigated during each scan at an amplitude of 5 mV (rms).

4. Ex situ FTIR-ATR measurements

The electrochemically synthesized poly(3,4-ethylenedioxythiophene), PEDOT film on Au (working electrode) was rinsed with distilled water and dried on air for 2 days. The films were studied with ex situ attenuated total reflection Fourier transform infrared (ATR-FTIR) spectroscopy. A PerkinElmer 1605 FTIR spectrophotometer together with a horizontally oriented ATR (HATR) was used for collecting spectra of electropolymerized film. FTIR spectra with a 2-cm^{-1} resolution in a wavenumber range from 650 to 4,400 cm^{-1} were recorded. Each spectrum was calculated as the average of 64 coadded spectra. The ZnSe internal reflection element (IRE) was attached to the external surface of the polymer film on one of the coated sides of former working electrode. The mechanical contact between ZnSe IRE and the sample was ensured by exerting pressure through a thick teflon sheet to the surface of gold sheet applying a physical clamping device. The HATR accessory was purged with nitrogen. The spectrum of empty ZnSe surface was

chosen as reference spectrum. The films formed were overoxidized or non-oxidized before drying process started.

Results and discussion

Cyclic voltammograms and stress change vs. electrode potential curves

As we have discussed in the "Introduction," the bending beam method offers the possibility to measure the changes of the stress in a thin polymer film [18–20]. Unfortunately, as with many electrochemical processes, the situation is more complex than it first appears. It is important to keep in mind that the original bending beam theory treats the thin layer on the substrate as a uniform entity. It is well known, however, that polymer films have complex internal structure. For instance, if pores are present in the film, the electrolyte may contact the underlying metal layer at the bottom of the pores. In this case the change in the surface stress of the metal/solution interface with electrode potential (E) occurs simultaneously with the change of the film stress. Both processes can result in the bending of the beam [20–22, 30], i.e., the radius of curvature of the strip (R) changes. The contributions from surface and bulk cannot be easily separated in the general case, therefore only the ΔR^{-1} vs. E (change in the reciprocal radius of curvature vs. electrode potential) plots ("voltdeflectograms") are given in the relevant figures. It has been reported that in some polymer/metal systems the polymer film completely blocks the metal surface (see, e.g., Refs. [39, 40]). The situation is expected to be somewhat simpler in these cases.

Porous layers

PPD films on gold or platinum are typical examples of porous structures. These electrodes can be well described by the so-called "brush model" proposed by Inzelt and Láng [37, 38, 41]. In the IL-brush the polymer chains are linked to bundles (with a distribution of "short" and "long" chains) containing micropores or nanopores. The length of the two types of chains is markedly different; however, both the short and the long chains may show also a distribution of length. The polymer film does not cover the underlying metal substrate fully, although a part of the polymer chains strongly attached to the surface metal atoms. Between the bundles there are macropores of considerably greater cross-sections than that of the micropores. Both the macropores and micropores are filled by the solution of supporting electrolyte.

Results of the deflection (stress change) measurements for a gold|PPD|0.1 M sulfuric acid(aq) electrode at a sweep rate of ν=50 mV s^{-1} are presented in Fig. 2 (thickness of the polymer t_f≈0.8 μm). The insert shows the cyclic voltammograms of the evaporated gold layer immersed in 0.1 M sulfuric acid solution without (curve 1) and with the polymer film (curve 2). Curve 2 shows the peak characteristic for the PPD film at negative potentials and the oxygen adsorption region at positive potentials. The shapes of the ΔR^{-1} vs. E curves in Fig. 2 are very similar, i.e., the surface stress changes for the two electrodes are almost identical. Consequently, in this case the stress change in the polymer films does not influence significantly the response of the beam.

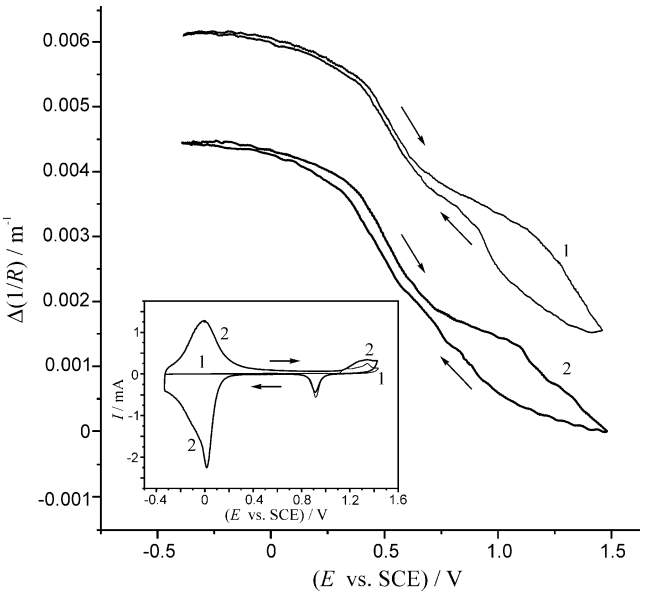

Fig. 2 Changes of the reciprocal radius of curvature ($\Delta(1/R)$) of the glass strip on side of it covered by a thin gold layer without (*1*) and with (*2*) a PPD layer on it. *Insert*: current I as a function of electrode potential E vs. SSCE at the sweep rate dE/dt=50 mV s^{-1} for gold (*1*) and gold covered by a PPD film (*2*) in c=0.1 mol·dm^{-3} H_2SO_4 solution

PEDOT films

The electromechanical properties of poly(3,4-ethylenedioxythiophene) thin films electrodeposited on gold-on-glass strips differ considerably from those of PPD|gold films. Cyclic voltammograms and $\Delta(1/R)$ vs. E curves recorded in 0.1 M Na_2SO_4 solution at different sweep rates (ν=10,20, 50,100 mVs^{-1}) are shown in Fig. 3a, b (thickness of the film t_f≈1.4 μm). The shapes of $\Delta(1/R)$ vs. E curves for PEDOT films are completely different from the shapes of the curves for uncovered gold or PPD covered gold. In addition, the change in R^{-1} in the same potential range is greater (in case of PEDOT the difference between the minimum and maximum is about 0.0045 m^{-1}, while for uncovered gold the corresponding value is 0.0027 m^{-1}), the hysteresis in the curves is pronounced and depends

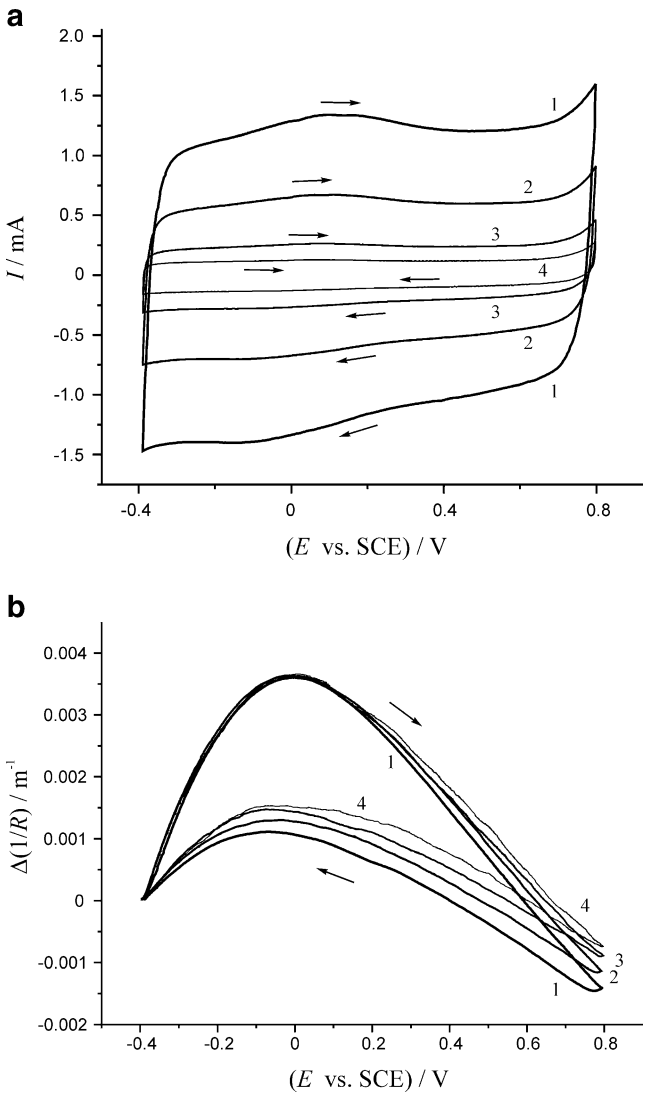

Fig. 3 **a** Cyclic voltammograms and **b** $\Delta(1/R)$ vs. E curves of poly (3,4-ethylenedioxythiophene) thin films electrodeposited on gold-on-glass strips, recorded in c=0.1 mol dm^{-3} Na_2SO_4 solution at different sweep rates. *1* ν=100 mVs^{-1}, *2* ν=50 mVs^{-1}, 3 ν=20 mVs^{-1}, *4* ν=10 mVs^{-1}

markedly on the sweep rate. All these observations suggest that stress changes in the polymer film may significantly contribute to the changes in R^{-1}, at least in the potential range from −0.4 to 0.8 V vs. SCE.

Oxidation of PEDOT films

Figure 4a shows cyclic voltammograms obtained for gold covered with electropolymerised PEDOT film (t_f≈0.7 μm) in 0.5 M sulfuric acid solution (ν=50 mV s^{-1}). The most pronounced feature in the potential range from −0.2 to 1.45 V vs. SCE is a broad oxidation peak at about 1.25 V with no corresponding reduction peak. The magnitude of the oxidation peak in the second CV recorded in the same potential range is significantly reduced. This decrease in the oxidation current and the absence of the reduction peak suggest that the oxidation process lead to irreversible changes in the polymer film. The overoxidation starts at about 0.8 V vs. SCE. Figure 4b shows in more detail the CV response in the range from −0.2 to 0.9 V vs. SCE before and after overoxidation. The CVs are similar in shape, but the redox capacity of the (over)oxidized polymer film is somewhat smaller than that of the freshly prepared film.

A series of cyclic voltammetric curves recorded for a gold|PEDOT|0.1 M sulfuric acid(aq) electrode (t_f≈1.4 μm) at a sweep rate of ν=50 mV s^{-1} are presented in Figs. 6a and 7a. The potential program applied to the electrode is given in Fig. 5. Two time intervals in Fig. 5 are marked by "A" and "B". The CVs shown in Fig. 6a were recorded in the time interval "A", the CVs in Fig. 7a in the time interval

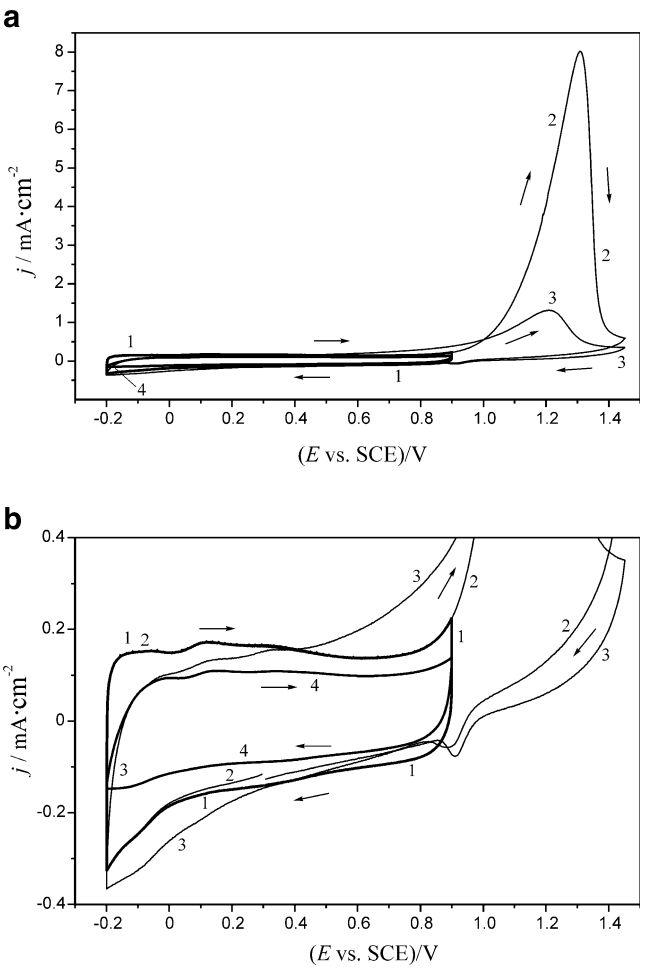

Fig. 4 **a** Cyclic voltammograms obtained for gold covered with electropolymerised PEDOT film in 0.5 M sulfuric acid solution before (curve *1*) and after (curve *4*) overoxidation. Curves *2* (first cycle in the potential range of −0.2 to 1.45 V vs. SCE) and *3* (second cycle) show broad oxidation peaks at about 1.25 V vs. SCE. (ν=50 mVs^{-1}). **b** Enlarged portions of the cyclic voltammograms

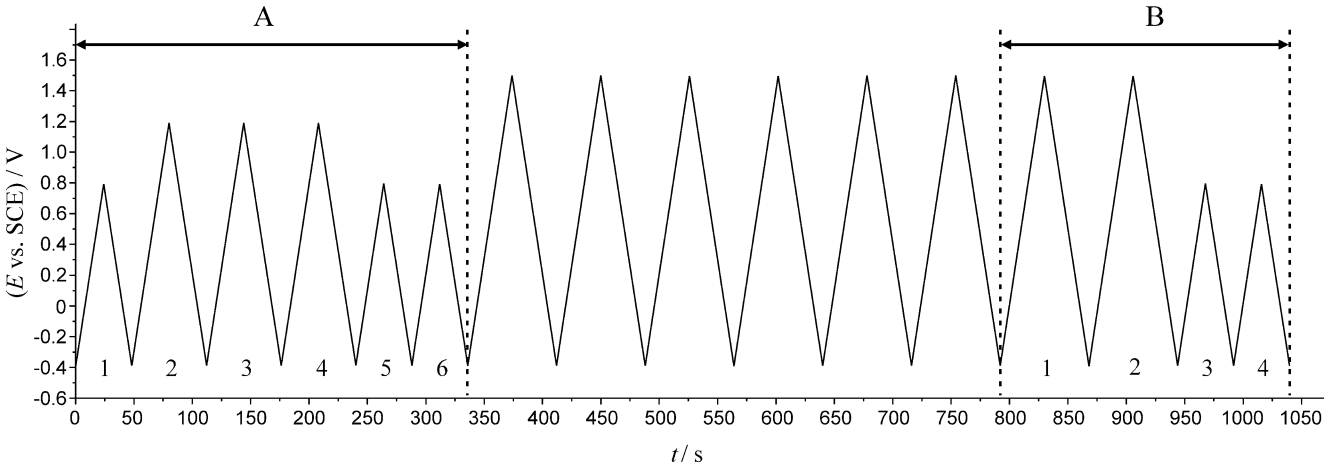

Fig. 5 Potential program applied to the Au|PEDOT|0.1 M sulphuric acid electrode. Sweep rates: ν=50 mV s^{-1}. "*A*" and "*B*" are time intervals during which the cyclic voltammetric curves and voltdeflectograms presented in Figs. 6a–b and 7a–b were recorded

"B". The corresponding $\Delta(1/R)$ vs. E curves are plotted in Figs. 6b and 7b.

The oxidation–reduction process is reversible, if the positive potential limit is kept below a critical value. According to the results, irreversible oxidation of the PEDOT film starts at or above 0.8 V vs. SCE. The shapes of the $\Delta(1/R)$ vs. E curves change considerably (curves 2–4 in Fig. 6b) if the electrode potential exceeds this value. The shape of the voltdeflectograms recorded after overoxidation (curves 5–6 in Fig. 6b) is similar to that recorded before overoxidation (curve 1 in Fig. 6b), however, the changes in $1/R$ are smaller in the same potential range. On the other hand, there are only slight differences between voltammograms of the "original" (curve 1 in Fig. 6a) and "oxidized" electrodes (curves 5–6 in Fig. 6a).

The changes in the $\Delta(1/R)$ vs. E curves become more and more pronounced with the increase of the number of cyclic voltammograms recorded in the potential range where overoxidation of the polymer occurs (Fig. 7b), and the shape of the curve begins to resemble more and more that of the ΔR^{-1} vs. E curve for the bare gold (curves 1–2 in Fig. 7b). These differences suggest that the film undergoes a degradation process of some sort upon its overoxidation above 0.8 V. After the application of eight potential cycles up to 1.5 V vs. SCE, the difference between the minimum and maximum values of ΔR^{-1} in the potential range from −0.4 to 0.8 V vs. SCE is less than about 0.001 m^{-1} (curves 3–4 in Fig. 7b). This is significantly smaller than the corresponding value (≈0.0045 m^{-1}) for the freshly prepared film (curve 1 in Fig. 6a). In this potential region the $\Delta(1/R)$ vs. E curve is of a very characteristic shape with a local maximum and a local minimum indicating that the polymer layer is still present on the gold surface. The same conclusion can be drawn on the basis of cyclic voltammetry. When the

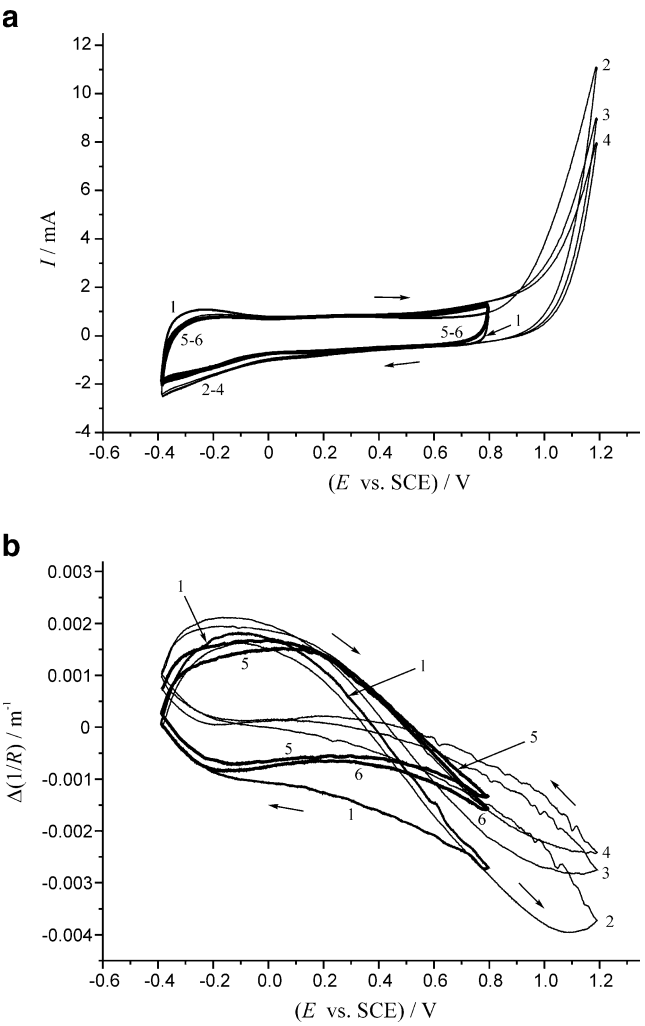

Fig. 6 **a** The series of cyclic voltammetric curves recorded in the time interval "*A*" in Fig. 5. **b** The simultaneously recorded $\Delta(1/R)$ vs. E curves

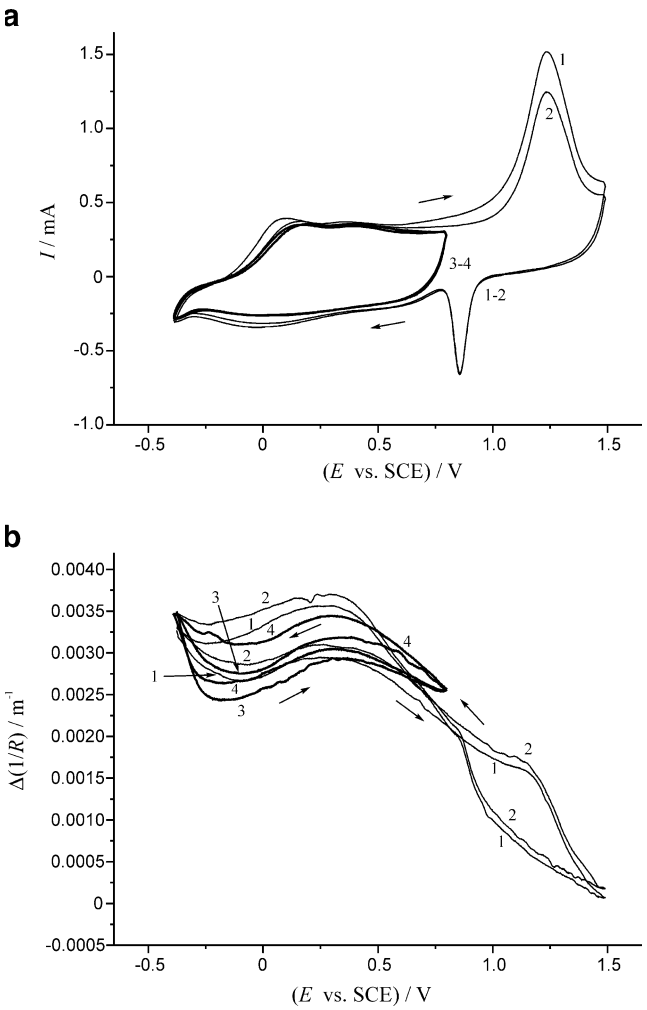

Fig. 7 **a** The series of cyclic voltammetric curves recorded in the time interval "*B*" in Fig. 5. **b** The simultaneously recorded $\Delta(1/R)$ vs. E curves

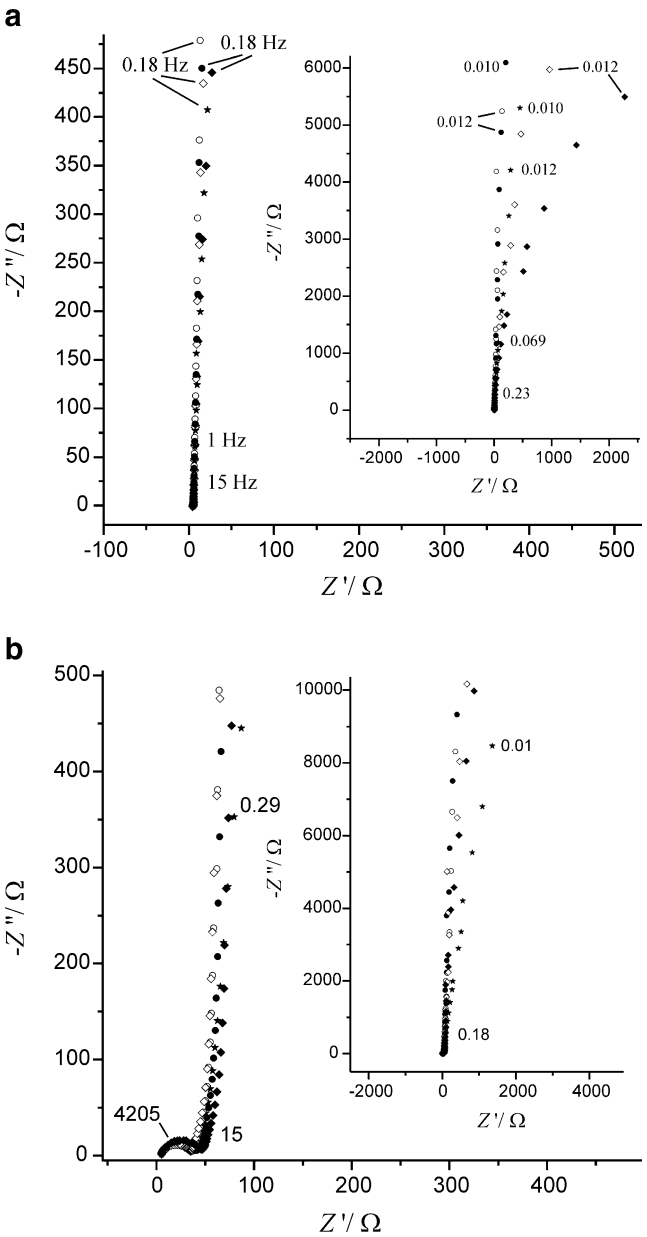

Fig. 8 **a** Impedance spectra (complex plane plots) of freshly prepared Au/PEDOT in 0.5 M H_2SO_4 solution at different electrode potentials. *stars*, E=0.10 V vs. SCE; *filled circles*, E=0.30 V vs. SCE; *empty circles*, E=0.40 V vs. SCE; *empty diamonds*, E=0.70 V vs. SCE; *filled diamonds*, E=0.80 V vs. SCE; **b** impedance spectra of the (over) oxidized film in 0.5 M H_2SO_4 solution at different electrode potentials. *Stars*, E=0.05 V vs. SCE; *filled circles*, E=0.20 V vs. SCE; *empty circles*, E=0.35 V vs. SCE; *empty diamonds*, E=0.50 V vs. SCE; *filled diamonds*, E=0.65 V vs. SCE

positive potential limit was extended until 1.5 V the cyclic voltammetric wave characteristic of gold oxide reduction appeared after a few cycles in the negative-going potential scan (curves 1–2 in Fig. 7a). On the other hand, the CVs recorded in the potential range from −0.4 to 0.8 V vs. SCE clearly show the presence of a significant amount of polymer in direct (electrical) contact with the gold surface (curves 3–4 in Fig. 7a), but the intensity of the redox response has diminished, compared with that in Fig. 6a.

Impedance spectra

In Fig. 8a impedance spectra (complex plane plots) of freshly prepared Au/PEDOT in 0.5 M H_2SO_4 solution at different electrode potentials are shown (t_f≈0.7 μm, geometric area≈1 cm^2). In the frequency range 0.1 Hz–10 kHz and at electrode potentials ranging from 0.1 to 0.7 V vs. SCE the impedance spectra indicate an almost purely capacitive behavior (the "low frequency capacity" of the film is C_L≈2.9 mF cm^{-2} at 0.1 V vs. SCE and C_L≈ 2.7 mF cm^{-2} at 0.4 V vs. SCE). However, at electrode potentials E>0.7 V vs. SCE the "semicircle" indicates that an interfacial charge transfer process has become fast enough to be observed (see insert of Fig. 8a). This process

Table 1 Comparison between band positions arising in PEDOT films in different electrochemical pretreatment

$\tilde{\nu}$(non-ox) cm^{-1}	$\tilde{\nu}$(ox)cm^{-1}	Reference data	Assignment	Remarks
1,511	1,516	1,513 [43]	ν_{as}(C=C) ring (thiophene)	ox. ind.
1,476	1,475	1,454 [43]	ν_{s}(C=C) ring (tiophene)	
1,398	1,405	1,394 and 1,370 [43]	ν(C–C) ring	
1,351(sh)	1,358	1,366 [44]	ν(C–C)	
1,314	1,326 (sh)	1,319 [45]		ox. ind.
1,184	1,194	1,183 [43]	ν(C–C) ring and ν(–$COCH_2CH_2OC$–)	
		1,195 [45]		ox. ind.
1,138	1,131	1,144–1,128 [43]	ν(–$COCH_2CH_2OC$–)	
1,087	1,094	1,093–1,176 [43] and 1,090 [45]	ν(–$COCH_2CH_2OC$–)	ox. ind.
1,044	1,055	1,052–1,047 [43] and 1,060 [45]	ν(–$COCH_2CH_2OC$–)	ox. ind.
1,012 (sh)	1,012 (sh)			
971	979	980		ox.ind.
919	937	943–930 [43]	ν(C–S) ring	
830	840	830 [43] and 849	ν(C–S) ring	ox.ind.

ox. ind. increase during the oxidation process, ν stretching, *sh* shoulder

can most probably be attributed to the slow degradation of the PEDOT film.

As it can be seen from Fig. 8b, the impedance spectra of overoxidized PEDOT on gold differ from those measured for freshly prepared Au/PEDOT. The film was oxidized by cycling the potential between −0.4 and 1.5 V vs. SCE. The most interesting feature is the appearance of an arc (or a "depressed semicircle") at high frequencies in the complex plane impedance plot. The "low frequency capacity" of the degraded film is about 2 mF cm^{-2} at 0.35 V vs. SCE. Studies addressing these issues are in progress.

Ex situ FTIR-ATR spectra of PEDOT films on gold

In order to gain some insight into the nature of the molecular level changes involved in the degradation process ex situ FTIR-ATR spectra were recorded before and after overoxidation of the PEDOT film.

The ATR intensity of solids depends strongly on the mechanical contact between the sample and IRE [42], i.e., increasing the pressure on amorphous PEDOT layer, more and more polymer chains immerse into the region of IR photon penetration depth.

When applied pressure difference on two individual spectrums is small, the spectral absorbance differences fit on a horizontal line. This was valid for both differently pretreated films ("freshly made" and overoxidized, $t_f \approx$ 1.4 μm) showing that the mechanical distortion has no influence on spectral properties.

Both samples investigated were exposed to air during 3 days drying to avoid the presence of variable amount of water in the samples producing overlapping bands, e.g., near 1,620 cm^{-1} (water deformation band). The band position data collected in Table 1 show only a slight difference compared to reference data. Reference data are taken from in situ ATR-FTIR spectroelectrochemical experiments [43–45] where acetonitrile was used as a solvent. It is interesting to note that for in situ ATR-FTIR difference spectra spectral bands at 1,513, 1,319, 1,195, 1,090, 1,060, 980, and 849 cm^{-1} were observed to be growing during electrochemical oxidation [45]. All the seven bands are observed in our FTIR-ATR spectra.

The more compact the film (attached to the ZnSe plate), the higher the spectral intensity of a particular vibration. The spectrum of polymer prepared without p-doping shows gradually decreasing intensity toward higher wavenumbers,

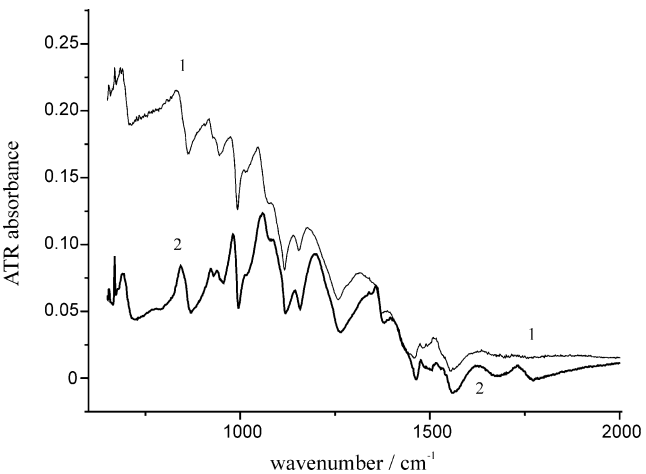

Fig. 9 Ex situ IR spectra of non-oxidized (*1*) and overoxidized (*2*) PEDOT film

while for the spectrum of overoxidized polymer such a behavior has not been observed (see Fig. 9). If the electrochemical polymer formation and subsequent oxidation result in different morphology of films the intensity change can be explained by density differences between the two films with different morphology.

Conclusions

The electrochemical bending beam method seems to be a useful tool for the in situ monitoring of the degradation of polymer films in electrochemical systems. Unfortunately, the change in the surface stress of the metal with electrode potential (E) occurs simultaneously with the change of the film stress. Both processes can lead to a change of the radius of curvature of the beam. The separation of the two contributions is the scope of future work.

Most of the experimental results can be explained based on the assumption that the observed electrochemical-mechanical behavior of the Au|PEDOT|0.1 M sulfuric acid (aq) electrodes before and after overoxidation is directly related to the internal structure of the polymer, i.e., by supposing structural changes in the originally compact and strongly adherent polymer film during the overoxidation (degradation) process. An alternative explanation is that during overoxidation the film gradually delaminates from the gold layer, exposing the underlying gold substrate to the electrolyte solution.

Acknowledgments Financial support from the Hungarian Scientific Research Fund (grants OTKA-67994/OMFB-01078/2007, OTKA-PD75445) are gratefully acknowledged. The authors thank National Instruments Europe Ltd. for the donation of data acquisition cards.

References

1. Lang U, Naujoks N, Dual J (2009) Synthetic Met 159:473–479
2. Wang GF, Tao XM, Wang RX (2008) Nanotechnology 19:145201
3. Lilliedala MR, Medforda AJ, Madsena MV, Norrmana K, Krebs FC (2010) Sol Energ Mat Sol C 94:2018–2031
4. Nasybulin E, Wei S, Cox M, Kymissis I, Levon K (2011) J Phys Chem C 115:4307–4314
5. Scott JC (2004) Science 304:62–63
6. Möller S, Perlov C, Jackson W, Taussig C, Forrest SR (2003) Nature 426:166–169
7. Cui X, Martin DC (2003) Sensor Actuat B-Chem 89:92–102
8. Vázquez M, Danielsson P, Bobacka J, Lewenstam A, Ivaska A (2004) Sensor Actuat B-Chem 97:182–189
9. Bobacka J (1999) Anal Chem 71:4932–4937
10. Drillet JF, Dittmeyer R, Jüttner K, Li L, Mangold KM (2006) Fuel Cells 6:432–438
11. Drillet JF, Dittmeyer R, Jüttner K (2007) J Appl Electrochem 37:1219–1226
12. Bobacka J, Lewenstam A, Ivaska A (2000) J Electroanal Chem 489:17–27
13. Yamato H, Ohwa M, Wernet W (1995) J Electroanal Chem 397:163–170
14. Sakmeche N, Aeiyach S, Aaron JJ, Jouini M, Lacroix JC, Lacaze PC (1999) Langmuir 15:2566–2574
15. Zykwinska A, Domagala W, Pilawa B, Lapkowski M (2005) Electrochim Acta 50:1625–1633
16. Du X, Wang Z (2003) Electrochim Acta 48:1713–1717
17. Pigani L, Heras A, Colina A, Seeber R, Lopez-Palacios J (2004) Electrochem Comm 6:1192–1198
18. Pei Q, Inganaes O (1992) J Phys Chem 96:10507–10514
19. Pei Q, Inganaes O (1993) J Phys Chem 97:6034–6041
20. Tabard-Cossa V, Godin M, Grütter P, Burgess I, Lennox RB (2005) J Phys Chem B 109:17531–17537
21. Láng GG (2008) In: Bard AJ, Inzelt Gy, Scholz F (eds) Electrochemical Dictionary. Springer, Berlin, pp 43–44
22. Láng GG, Sas NS, Vesztergom S (2009) Chem Biochem Eng Q 23:1–9
23. Ueno K, Seo M (1999) J Electrochem Soc 146:1496–1499
24. Sahu SN, Scarminio J, Decker F (1990) J Electrochem Soc 137:1150–1154
25. Cattarin S, Pantano E, Decker F (1999) Electrochem Commun 1:483–487
26. Cattarin S, Decker F, Dini D, Margesin B (1999) J Electroanal Chem 474:182–187
27. Raiteri R, Butt H-J Grattarola M (1998) Scanning Microscopy 12:243–254
28. Kongstein OE, Bertocci U, Stafford GR (2005) J Electrochem Soc 152:C116–C123
29. Stafford GR, Bertocci U (2006) J Phys Chem B 110:15493–15498
30. Godin M, Tabard-Cossa V, Miyahara Y, Monga T, Williams PJ, Beaulieu LY, Lennox B, Bruce R, Grütter P (2010) Nanotech 21:075501
31. Stoney GG (1909) Proc Roy Soc London A32:172–175
32. Láng GG, Ueno K, Ujvári M, Seo M (2000) J Phys Chem B 104:2785–2789
33. Láng GG, Seo M (2000) J Electroanal Chem 490:98–101
34. Láng GG (2010) J Appl Phys 107:116104
35. Stoyanova A, Tsakova V (2010) J Solid State Electrochem 14:1947–1955
36. Poppendieck W, Hoffmann KP (2009) In: Vander Sloten J, Verdonck P, Nyssen M, Haueisen J (eds) ECIFMBE 2008, IFCMBE Proceedings 22, Springer, Heidelberg, pp 2409–2412
37. Láng GG, Ujvári M, Rokob TA, Inzelt G (2006) Electrochim Acta 51:1680–1694
38. Láng G, Ujvári M, Inzelt G (2001) Electrochim Acta 46:4159–4175
39. Kazarinov VE, Levi MD, Skundin AM, Vorotyntsev MA (1989) J Electroanal Chem 271:193–211
40. Vorotyntsev MA, Graczyk M, Lisowska-Oleksiak A, Goux J, Moise C (2004) J Solid State Electrochem 8:818–827
41. Inzelt G, Láng GG (2010) In: Cosnier S, Karyakin A (eds) Electropolymerization. Wiley, Weinheim, pp 51–76
42. Mirabella FM Jr (ed) (1993) Internal reflection spectroscopy, Practical spectroscopy series vol. 15. Marcel Dekker, New York, p 33
43. Kvarnström C, Neugebauer H, Blomquist S, Ahonen HJ, Kankare J, Ivaska A (1999) Electrochim Acta 44:2739–2750
44. Garreau S, Louarn G, Buisson JP, Froyer G, Lefrant S (1999) Macromolecules 32:6807–6812
45. Kvarnström C, Neugebauer H, Ivaska A, Sariciftci NS (2000) J Mol Struct 521:271–277